Response of A Large Sensitive Volume Lithium-Drifted Silicon Detector to Gamma and Beta Rays

Sakae NISHIU*

Shimizu Laboratory, Institute for Chemical Research, Kyoto University

Received January 17, 1966

The construction and characteristics of a large sensitive volume lithium-drifted silicon detector are reported. Its spectroscopic response for gamma and beta rays, especially photoelectric absorption peaks and Compton electron distributions are discussed comparing with that of a NaI (Tl) scintillator. In contrast with lithium-drifted germanium detectors, silicon detectors have lower counting efficiency, but have the merit of being able to be stored at room temperature when it is not in use. Using these characteristics combined with its excellent energy resolution and anti-coincidence counting method, there will be new gamma ray spectroscopic applications in large sensitive volume silicon detectors in despite of its low counting efficiency.

I. INTRODUCTION

In the previous report[1], we described the possibility of the spectroscopic measurement of low energy gamma rays by the photoelectric absorption of small lithium-drifted silicon detectors (45mm^2 in area and about 2mm in sensitive depth).

Here we report the response of a thick silicon detector for gamma rays and high energy electrons. It can be inferred from recent reports[2] that lithium-drifted germanium detectors have good energy resolution and higher counting efficiency than silicon detectors, and wide applications for gamma-ray energy measurement are expected. They have as very high resolution of energy as silicon detectors compared with scintillation detectors such as NaI(Tl). But, germanium detectors must be cooled under the dry ice temperature even when it is not in use and considered to be rather articles of consumption.

II. CONSTRUCTION

To increase the counting efficiency, we tried to make detectors of much more sensitive volume than that reported previously. As floating-zoned silicon ingots usually available are a little over 20 mm in diameter, detector size was designed 20mm in effective diameter, and about 5mm in sensitive layer thickness.

Two methods were used to estimate the depth of the intrinsic layer of the detector thus made. First, the distribution of resistivity was observed by the four points probe method[3] along the periphery side from the surface of p-side to that of n-side through which lithium is diffused. The resistivity profile is shown

* 西宇　栄, Also at Takarazuka Radiation Laboratory, Sumitomo Atomic Energy Industries Ltd., Takarazuka.

in Fig. 1. Secondly, potential distribution was also measured similarly about the same detector with the reverse bias voltage applied (Fig. 2). By these two observations it is evident that the intrinsic depth and p-side dead layer thickness is bout 4.5 and 1mm, respectively, and the dead layer thickness of n-side surface is negligibly small. The error of measurements of the resistivity is very large in high resistivity silicon, and strictly speaking, the edge correction[3] must be carried out with the curve shown in Fig. 1, but there is almost no change in the data mentioned above.

On the technique of the detector preparation, there is no difference from that reported[1] in principle, but for a thick detector a very long drift time is needed, at least from 7 to 10 days and moreover "the clean up treatment[4]" must be carried out at the last stage of drift process. Without this treatment, the depletion layer thickness is very small compared with the usual simple drift theory and depends upon voltage applied.

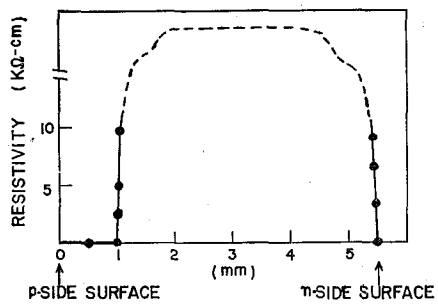

Fig. 1. Resistivity profile in the lithium-drifted silicon detector.

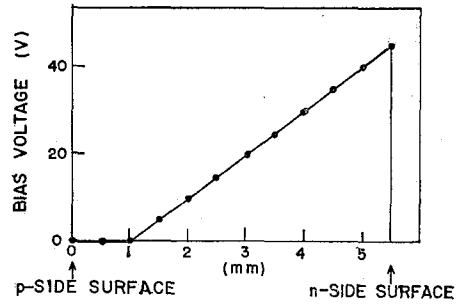

Fig. 2. Potential distribution in the lithium-drifted silicon detector with the backward bias voltage.

III. DETECTION PERFORMANCE

Lithium-drifted silicon detectors with large sensitive volume had to be cooled to decrease the backward leakage current owing to the thermal generation. By cooling the detector from room to liquid nitrogen temperature the backward leakage current was easily lowered by two orders of magnitude, decreasing below 10^{-8} amperes with the backward bias voltage of 100 volts. All measurements of gamma rays were carried out in the simple cryostat, shown in Fig. 3. The gamma-ray sources used here are needed to be several times stronger in activity than that generally used with NaI (Tl) scintillators. Gamma-ray sources of about several microcuries, varying with the gamma-ray energy of course, were used but severe caution was taken to avoid the pile-up effects of the signal.

In Figs. 4~9, gamma-ray spectra of various sources up to 1.33 MeV in energy are shown, measured by the large sensitive volume silicon detector described above with an aluminium foil or beryllium plate as an absorber of beta particles or internal conversion electrons when needed. The relation between the pulse height of photoelectric absorption peak and its energy is plotted in Fig. 10, showing a very good linearity in all range. The sensitive layer of this detector is suffi-

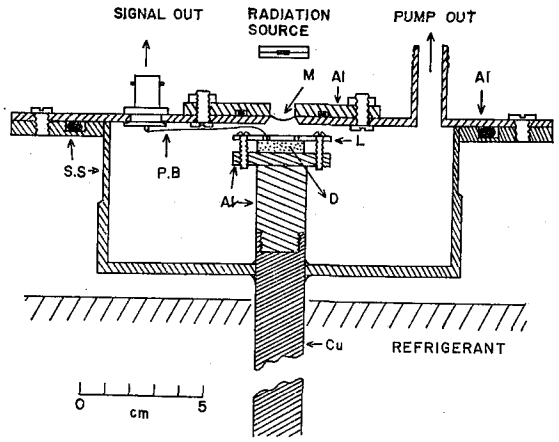

Fig. 3. A vacuum chamber to cool the detector mainly for the measurement of gamma rays. D - detector, S.S - stainless steel, P.B - phospher bronze, M - myler sheet (6μ in thickness), L-Lucite plate.

ciently thick for the photoelectrons and the window layer of n-side surface from which radiations are introduced is negligible for gamma rays. There is no window effect as that in measurements of alpha or beta particles. The relations shown in Fig. 10 can be used as a calibration standard of the actual energy liberated in the depletion layer of silicon detectors, regardless of kinds of incident ionizing particles.

As a comparison of Fig. 6, a gamma-ray spectrum from ^{125}Sb was measured by a $3''\phi \times 3''$ NaI (Tl) scintillator, as shown in Fig. 11. In these two spectra, distinct differences are observed in several points : (1) The single peak in Fig. 11 due to photoelectric absorption of 0.637 and 0.595 MeV gamma rays is perfectly resolved into two peaks in Fig. 6, (2) on the contrary the peak due to 0.430 and 0.463 MeV

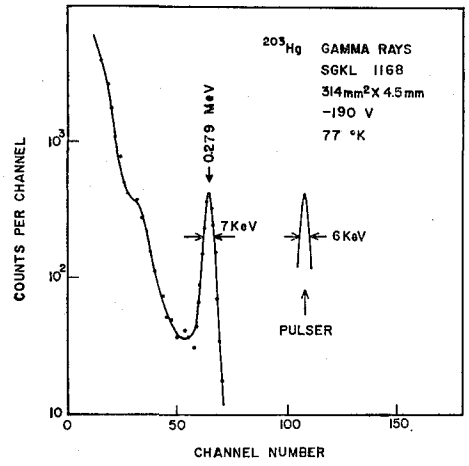

Fig. 4. Gamma-ray spectrum from ^{203}Hg observed with a large sensitive volume silicon detector at 77°K.

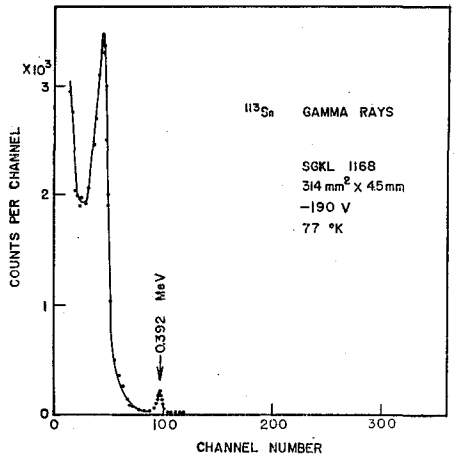

Fig. 5. Gamma-ray spectrum from ^{113}Sn observed with a large sensitive volume silicon detector at 77°K.

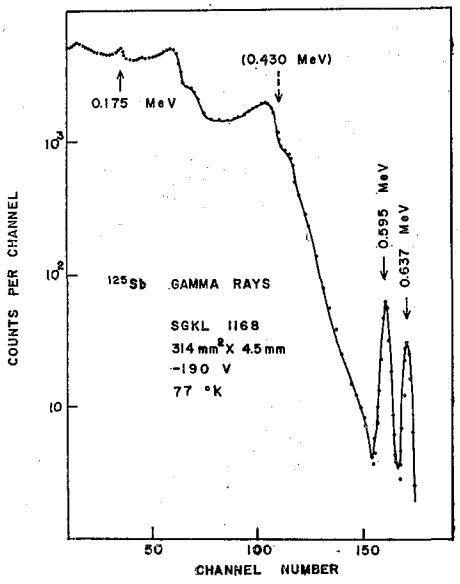

Fig. 6. Gamma-ray spectrum from ^{125}Sb observed with a large sensitive volume silicon detector at 77°K.

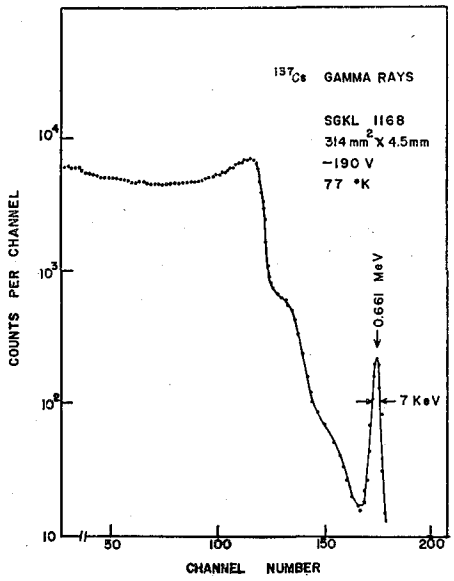

Fig. 7. Gamma-ray spectrum from ^{137}Cs observed with a large sensitive volume silicon detector at 77°K.

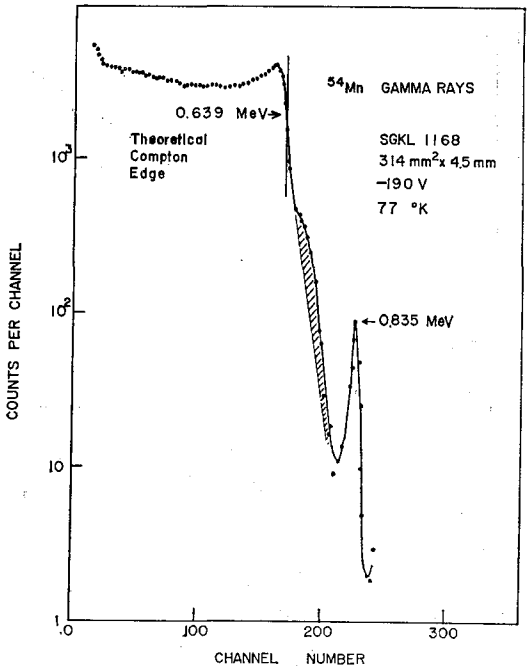

Fig. 8. Gamma-ray spectrum from ^{54}Mn observed with a large sensitive volume silicon detector at 77°K.

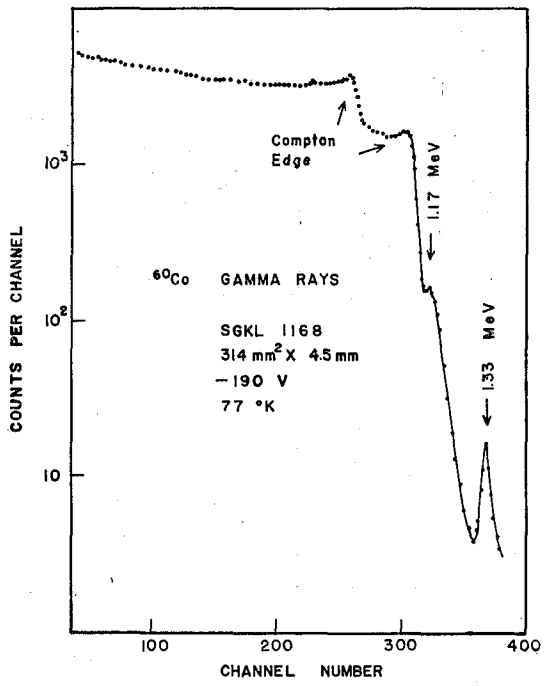

Fig. 9. Gamma-ray spectrum from ^{60}Co observed with a large sensitive volume silicon detector at 77°K.

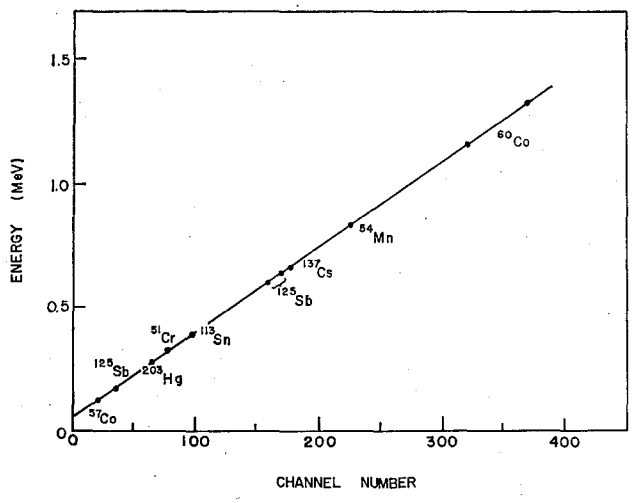

Fig. 10. Pulse-height response of a large sensitive volume silicon detector to gamma rays at 77°K.

gamma rays is completely vanished in the latter under the Compton electrons of the higher energy gamma rays and (3) the peak due to 0.175 MeV gamma rays is only slightly recognizable. In Fig. 9, the peak of the lower energy gamma rays from ^{60}Co is barely recognizable at the Compton edge of 1.33 MeV gamma rays.

As shown in Figs. 4 and 7, the full width half maximum (FWHM) of photo-electric absorption peak is about 7 KeV, giving the energy resolution of 1% for 0.661 MeV gamma rays from ^{137}Cs. The FWHM for the amplifier system[1] alone amounts to 6 KeV.

When Compton electrons are mostly rejected by the anti-coincidence counting method, all photopeaks will be catched with high resolution, impossible for the scintillator, and important applications will be expected.

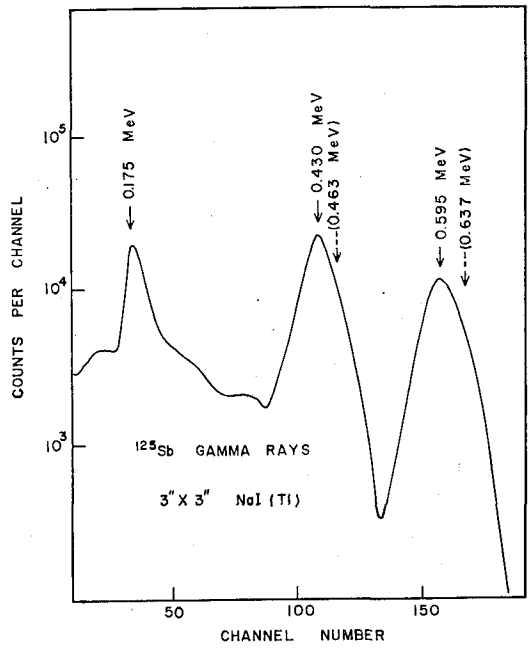

Fig. 11. Gamma-ray spectrum from ^{125}Sb observed with a $3'' \phi \times 3''$ NaI (Tl) scintillator.

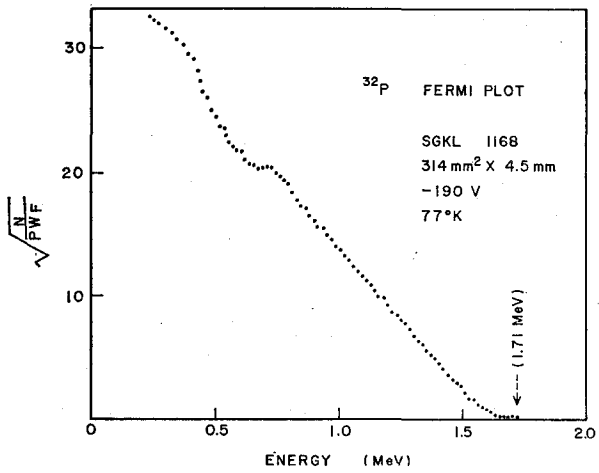

Fig. 12. Fermi plot of the beta-ray spectrum of ^{32}P observed with a large sensitive volume silicon detector at 77°K.

In the previous report[1], we carried out "Fermi plot" and showed that there was more or less straight part on the high energy end of the plot in several beta-emitting nuclei. The maximum energy was decided from it except in the case of ^{32}P. As for ^{32}P, the maximum-energy electrons penetrate through the sensitive layer and no straight part was seen in the high energy end of the plot. In this work, we again practiced the Fermi plot with the thick detector enough for all beta particles of ^{32}P (Fig. 12). But, also with this detector, we conlol scarcely recognize linear part on the high energy end. In this case, despite of its ample thickness, it seems necessary to correct the beta-ray spectrum for back-scattering electrons to find out the precise maximum energy from the Fermi plot.

IV. DISCUSSION

IV.1. Peak-to-Total Ratio of the Gamma-Ray Spectrum

In the spectra shown above, it is readily noticed that the photoelectric absorption peak is very low compared with the spectrum of Compton electrons. Quantitative discussions are tried here about gamma-ray spectrum from ^{54}Mn, which emits monochromatic gamma rays and have the well known decay scheme. Internal bremsstrahlungs and X rays from the source are neglected and all scattered photons from the wall of the cryostat are not considered in this rough estimation. The experimental peak-to-total ratio R of the spectrum shown in Fig. 8 was obtaimed by the extrapolation of the curve of the low energy part hidden under the noise as

$$R=0.00098\pm0.00002\ ,$$

which is only one five-hundredth of 0.47, the experimental peak-to-total ratio of the spectrum measured by a $3''\phi\times3''$ NaI (Tl) scintillator at the same distance from the gamma-ray source. The theoretical peak-to-total ratio R' for the 0.835 MeV gamma rays from ^{54}Mn incident upon our silicon detector, computed by the narrow beam approximation neglecting the secondary interactions using the table of gamma-ray absorption coefficients given by Storm *et al*[5], is given by

$$R'=0.00087.$$

Comparing these two data, about 11% of total counts in the photopeak in Fig. 8 results from the secondary interactions of Compton scattered photons. Because the theoretical value of photoelectric absorption coefficient is given only as one figure, these estimations are rather rough. Intrinsic efficiency given by the ratio of numbers of interacted photons to total photons incident upon the detector is about 7.1%.

IV.2. Energy Spectrum of Compton Electrons

The ordinate of the Fig. 8 is shown in linear scale in Fig. 14 by the dotted line, showing the characteristic spectrum of Compton electrons, which we will treat here theoretically. Using the signs in Fig. 13,

$$\cot\varphi=(1+\alpha)\tan\frac{\theta}{2}. \qquad (1)$$

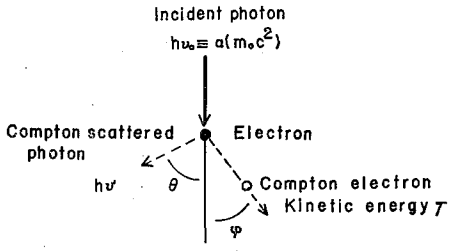

Fig. 13. Trajectories in the scattering plane for the incident photon, the scattered photon, and the scattering electron which receives kinetic energy. For the gamma rays from ^{54}Mn $\alpha=1.634$. For $\theta=90°$, $\varphi=20°\ 47'$ and $T=0.317$ MeV.

The collision cross section σ per electron produced by unpolarized photons per unit energy interval of the recoiled electron is given by the relation[6] :

$$\frac{d\sigma}{dT}=\frac{\pi r_0^2}{\alpha h\nu_0}\left(\frac{\nu'}{\nu_0}\right)^2\left(\frac{\nu_0}{\nu'}+\frac{\nu'}{\nu_0}-\sin^2\theta\right)\left[\frac{(1+\alpha)^2-\alpha^2\cos^2\varphi}{(1+\alpha)^2-\alpha(2+\alpha)\cos^2\varphi}\right]^2, \tag{2}$$

where r_0=classical electron radius 2.818×10^{-13}cm,

$\alpha\equiv h\nu_0/m_0c^2$,

m_0=rest mass of electron.

Using these relation for $\varphi=0°\sim90°$, theoretical cross section for 0.835 MeV gamma rays is shown by the solid line in Fig. 14. In the same figure, the

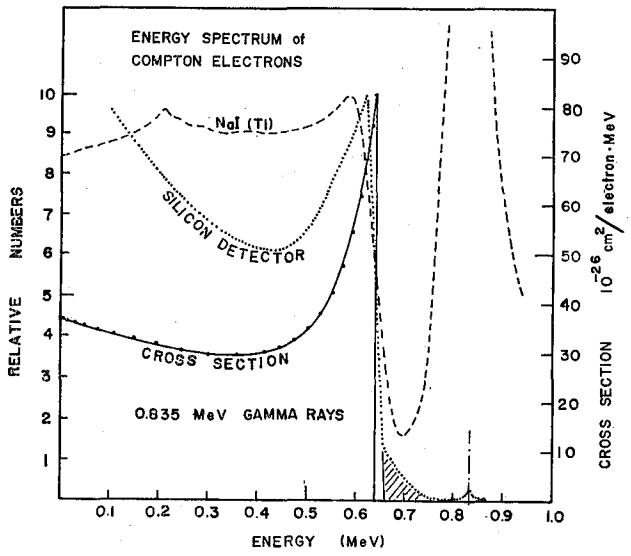

Fig. 14. Number-energy spectrum of Compton electrons produced by primary photons of 0.835 MeV gamma rays from ^{54}Mn (solid line) and the gamma-ray spectrum measured by a large sensitive volume silicon detector (dotted line) and a $3''\phi\times3''$ NaI (Tl) scintillation detector (broken line), respectively. Some of the photons scattered successively twice in the sensitive region of the silicon detector gives up the energy more than 0.639 MeV and are associated with the hatched part.

spectrum of gamma rays from ^{54}Mn measured by a $3''\phi\times3''$ NaI (Tl) scintillator is plotted by the broken line. The height of Compton edges of these curves are normalized for comparison. As shown in this figure, the spectrum measured by the silicon detector is much more similar especially near the Compton edge, to that of the theoretical cross section, compared with that measured by the scintillator. This results from next three reasons :

(1) The energy resolution of the silicon detector is very high compared with that of the scintillator.

(2) The dimension of sensitive region of the silicon detector is enough small compared with the mean free path of the incident photon in silicon (61mm), or strictly speaking, that of the scattered photon (34~61mm).

(3) On the contrary, the dimension of the silicon detector is enough large compared with the maximum range of electrons scattered in silicon (0.9mm).

It is clear that the condition (1) and (3) are fulfiled with our detector. The condition (2) requires that there is no secondary interaction of scattered photons in the sensitive region. To survey the condition (2), we try some estimations. The probability P that the scattered photon be underging the second interaction in the sensitive region is estimated by the relation :

$$P=\frac{1}{4\pi}\int_{\Omega}\mathrm{d}\omega(1-\mathrm{e}^{-L/\lambda}), \tag{3}$$

where λ=mean free path of primarily scattered photon,

L=the path length through the sensitive region along an element of solid angle $\mathrm{d}\omega$ from the position of primary interaction.

Because L is the largest when $\theta=90°$, photons scattered at right angles to the direction of incident flux give the most contribution in integration (3). Nevertheless, P is not so much than 6%, and experimentarily, the hatched part in Fig. 8 or 13 is mainly due to a part of photons mentioned above, which interacted successively twice in sensitive region and consequently liberated more energy in all than 0.639 MeV (Compton edge of the 0.835 MeV gamma rays).

The conditions (1) and (2) mentioned above are not fulfiled in the spectrum measured by the scintillator, and the curve shown by the broken line departs considerably from that shown by solid line. The Compton edge measured by the silicon detector is pointed sharply, and rather should be called "the Compton peak". The backscattering peak at 0.196 MeV does not appear clearly in the silicon detector.

There is considerable departure between dotted and solid line at the lower energy side of the Compton spectrum. This comes partly from electrons runned away out of sensitive region and partly from photons scattered twice in the detector or from the wall of the cryostat.

IV.3. The Compton Edge

The energy of the Compton edge is given by the well known expression :

$$E=\frac{h\nu_0}{1+\dfrac{1}{2\alpha}}. \tag{4}$$

But it is not situated at the peak of the Compton spectrum as shown in Fig. 14 but rather shifted a little higher energy side. With a silicon detector having smaller sensitive volume (1cm^2 in area and 1.43mm in height) Baily *et al*[7] reported that the energy given by the expression (4) just coincide with that at the half height of the peak in the Compton spectrum measured by the lithium-drifted silicon detector. For our silicon detector with decuple sensitive volume, it is verified that there exists the same relation even for the 1.33 MeV gamma rays from ^{60}Co as that mentioned above with the smaller silicon detector. This fact will also be used for gamma-ray spectroscopy.

ACKNOWLEDGMENTS

The author would like to express his sincere thanks to Mr. T. Nakakado who prepared the detector, and to Y. Kamino and J. Murayama for their cooperations in the present work. Many valuable discussions with Professor S. Shimizu are also gratefully acknowledged.

REFERENCES

(1) S. Nishiu, T. Nakakado and S. Shimizu, *Bull. Inst. Chem. Res., Kyoto Univ.*, 42, 319 (1964).
(2) P. P. Webb and R. L. Williams, *Nucl. Instr. & Meth.*, 22, 361 (1963).
A. J. Tavendale and G. T. Ewan, *Nucl. Instr. & Meth.*, 25, 185 (1963).
(3) A. Uhlir Jr., *Bell Syst. Tech. J.*, 34, 105 (1955).
(4) J. W. Mayer, *J. Appl. Phys.*, 33, 2894 (1962).
(5) E. Storm, E. Gilbert and H. Israel, *USAEC Rpt. LA-2237* (Nov. 18, 1958).
(6) R. D. Evans, *"The Atomic Nucleus."*, p. 674, McGraw Hill Book Co. Inc., 1955.
(7) N. A. Baily, J. W. Mayer and R. J. Grainger, *I. R. E. Trans., Nucl. Sci.*, NS-9, No. 1, 91 (1962).